Geometric and electronic structures of (BeO)N (N = 2–12, 16, 20, and 24): Rings, double rings, and cages

Lei Ren, Longjiu Cheng, Yan Feng, and Xuemei Wang

Citation: J. Chem. Phys. **137**, 014309 (2012); doi: 10.1063/1.4731808
View online: http://dx.doi.org/10.1063/1.4731808
View Table of Contents: http://jcp.aip.org/resource/1/JCPSA6/v137/i1
Published by the American Institute of Physics.

Geometric and electronic structures of $(BeO)_N$ ($N = 2$–12, 16, 20, and 24): Rings, double rings, and cages

Lei Ren, Longjiu Cheng,[a] Yan Feng, and Xuemei Wang
School of Chemistry and Chemical Engineering of Anhui University, Hefei, Anhui 230039, People's Republic of China

(Received 19 March 2012; accepted 14 June 2012; published online 5 July 2012)

The structure of $(BeO)_N$ clusters ($N = 2$–12, 16, 20, and 24) are investigated using the method combining the genetic algorithm with density function theory. Benchmark calculation indicates that THSSh functional is reliable to predict the structures of $(BeO)_N$ cluster. The global minimum structures of $(BeO)_N$ clusters are rings up to $N = 5$, double rings at $N = 6$ and 7 and cages at $N \geq 8$. Besides, almost all of the structures of $(BeO)_N$ cluster are aromatic according to the NICS criterion. Adaptive natural density partitioning analysis reveals that C_6, $(BN)_3$, and $(BeO)_3$ rings (C_{24} and $(BeO)_{12}$ fullerenes) are similar in bonding patterns. The building-up principle of $(BeO)_N$ is different from that of covalent (BN) and ionic (LiF and MgO) clusters. © *2012 American Institute of Physics*. [http://dx.doi.org/10.1063/1.4731808]

I. INTRODUCTION

The structural question of a chemical system, both at micro and macro level, is one of the most fundamental challenges to chemists and physicists.[1,2] Atomic and molecular cluster is an intermediate stage between isolated atoms/molecules and bulk materials. The low-lying structural information of clusters can help us to understand the property evolution from micro- to macro-materials. The building-up principle of clusters is much different from that of crystals. Unfortunately, it is difficult to theoretically investigate the building-up principle and obtain those low-lying structures (especially for large size clusters), because the potential energy surfaces of clusters are quite complex with the increase of cluster size. Hence, it is interesting and challenging to investigate the structures of all kinds of clusters.

Binary clusters and nanoalloys are becoming a hot research topic because their novel properties which can be exploited for application in catalysis, electronics, and optics.[3] In fact, their properties and applications are closely related to their special structures. It is demonstrated that binary clusters often are in favor of rings,[4] cubic,[5] and cages,[6] and nanoalloys prefer icosahedra, polytetrahedra, and polyicosahedra.[7–12]

Alkali-earth oxide is an important class of metal oxides and the most of them crystallize in the cubic rock salt (NaCl) structure. But beryllium oxide is of hexagonal wurtzite crystal, the distance between Be and O atoms is very short and the interatomic piles are very tight. Therefore, beryllium oxide is a rare oxide which can be used in high resistance and high thermal conductivity of ceramic materials. Besides, beryllium and beryllium oxides are indispensable valuable materials in the atomic energy, rockets, missiles, aviations, and metallurgical industry. In fact, these popular application and excellent characteristics of BeO depends on its novel interaction between Be and O atoms. Be–O bond composes of covalent and ionic bond, but the covalent bond ratio (64%) is higher than that of ionic bond (36%).[13] It is highly probable that the structures of gas-phase BeO clusters are out of the ordinary, and clusters may inherit the novel properties of bulks. However, how beryllium oxide unit pile and what the cluster structures are like still remain questions.

In this paper, we performed an investigation on structures of $(BeO)_N$ ($N = 2$–12, 16, 20, and 24) clusters by a method combining the genetic algorithm (GA) and density functional theory (DFT). Our results show that the covalency of Be–O bond leads to $(BeO)_N$ clusters proposes of unique structures and properties, and the building-up principle of $(BeO)_N$ clusters is different from that of $(BN)_N$, $(LiF)_N$), and $(MgO)_N$ clusters.

II. COMPUTATIONAL DETAILS

A. Global optimization method

The calculations are carried out by combination of GA and DFT method. The GA was employed to search the potential energy surface directly using DFT method. And all DFT computations were accomplished by the GAUSSIAN 09 package[14] using the TPSSh functional.[15] The GA cannot promise to find the global minimum (GM) structure in one calculation, so for each case, 5 independent GA runs are carried out. In global research of the potential energy surface, a small basis set (3-21G) is used for saving time. After global optimization, the low-lying TPSSh/3-21G isomers are fully relaxed at TPSSh/6-311+G* level of theory.

B. Benchmark calculations

To verify the reliability of different functionals of DFT methods, a benchmark calculation is carried out by

[a]Author to whom correspondence should be addressed. Electronic mail: clj@ustc.edu.

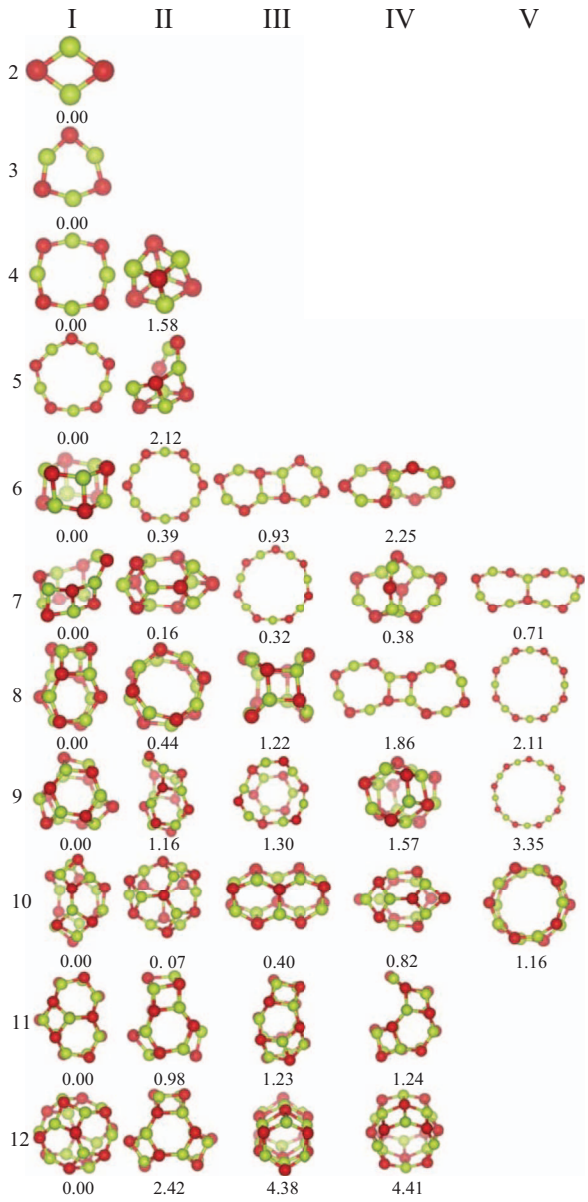

FIG. 1. Relevant structures of $(BeO)_N$ of $N = 2$–12. The structures in column **I** correspond to the global minima; columns **II**–**V** correspond to isomers (local minima) that are higher in energy, and the relative energies in eV are labeled in the figure. O-red; Be-green.

comparing the relative stability of the three isomers of $(BeO)_6$ (see structures in Figure 1). Results of the benchmark calculation are given in Table I to compare different functionals (TPSSh, PBE0,[16] M06,[17] B3LYP,[18] BPW91,[19,20] and BP86 (Refs. 21 and 22)) with the high-level coupled-cluster single double triple (CCSD(T)) (Ref. 23) method. Note that TPSSh and PBE0 functionals are consistent with CCSD(T) method in the energetic sequences of the three isomers. However, relative stability of the planar isomers (6**II** and 6**III**) is overvalued for M06, B3LYP, BPW91, and BP86 functionals (especially for B3LYP functional, where the relative energy of the monocyclic 6**II** is undervalued by even 1.3 eV). Thus, compared to CCSD(T) method, TPSSh functional is reliable for $(BeO)_N$ clusters in relative stability of different packings.

TABLE I. Comparison of single point energies for the three low-lying isomers of $(BeO)_6$ (see structures in Figure 1).[a]

Method	6**I**	6**II**	6**III**
CCSD(T)[b]	− 539.793569	0.52	0.99
TPSSh	− 540.787596	0.39	0.93
ZPE[c]	0.046128	− 0.11	− 0.08
PBE0	− 540.130683	0.27	0.87
M06	− 540.536804	− 0.46	0.35
B3LYP	− 540.802030	− 0.78	0.22
BPW91	− 540.673454	− 0.14	0.58
BP86	− 540.721861	− 0.14	0.57

[a]Energies for 6**I** are in atomic units, other energies are relative to this in eV. Results are single point energies with 6-311+G* basis sets for TPSSh/6-311+G* geometry.
[b]The basis set is aug-cc-pvtz for CCSD(T).
[c]Zero point energy at TPSSh/6-311+G*.

III. RESULTS AND DISCUSSION

A. Structures

Using the combination of genetic algorithm and DFT method, we obtained a series of relevant structures for $(BeO)_N$ clusters at the TPSSh/6-311+G* level. The structures can be divided into different families, namely, rings, double rings, triple rings, quad-rings, glasses, cages, and fullerenes (see Table II). Figure 1 plots the most relevant structures for $(BeO)_N$ ($N = 2$–12). The GM are monocyclic rings (up to $N = 5$) with D_{nh} symmetry, and the energy gap between the planar GMs and the 3D isomers is relatively large. 6**I** is a double ring and 6**III** is a glass-like structure containing two six-membered rings and one four-membered ring. The GM (7**I**) of $(BeO)_7$ is an analogue of double ring. Cage-like isomer (7**II**) is the most stable structure for $(LiF)_7$ (Ref. 24) and $(MgO)_7$.[25] Isomer 8**I** has a high symmetry (S_4). 9**I** and 10**II** are not found in other clusters. 11**I** is a chiral cage and 11**IV** is an open-shell structure. 12**I** is a fullerene-like cage of four- and six-membered rings.

Figure 2 displays the structures of $(BeO)_N$ at $N = 16$, 20, and 24. The GMs (16**I**, 20**I**, and 24**I**) are fullerene-like cages, and the other local minima are multiple-rings. Energy gaps between the fullerene-like cages and the multiple-ring structures are very large, and the value increases with the increase of the size (6.04 eV at $N = 16$, 7.36 eV at $N = 20$, and 13.18 eV at $N = 24$). At such cluster sizes, cubic structures are GM for MgO clusters.[26] For BeO clusters, however, the cubic structures are extremely high in energy (more than 20 eV) and not given in Figure 2. The majority of cages consist of 4- and 6-menbered rings, in which most of Be/O atom connects with three O/Be atoms.

B. Binding energy and stability

The calculated binding energies (the average interaction energy per BeO formula unit in the cluster) versus cluster sizes (the number of formula units in the cluster) are plotted for the GMs in Figure 3(a). It is clearly seen that the average binding energy increase with the growth of cluster size. To show the relative stability of the global minimum structures at different cluster size, the energies are depicted in

TABLE II. Family[a], electronic state, symmetry, and NICS value of structures for $(BeO)_N$ ($N = 2$–12) clusters.

N	Family	ES[b]	Symm[c]	Δ_{HL}[d]	NICS[e]	N	Family	ES	Symm	Δ_{HL}	NICS
2I	R	^1A_g	D_{2h}	3.99	−10.67	**8I**	C	^1A	S_4	6.36	−3.23
3I	R	$^1A_1'$	D_{3h}	6.14	−4.64	**9I**	C	$^1A'$	C_{3h}	6.53	−2.08
4I	R	$^1A_{1g}$	D_{4h}	6.24	−0.99	**9II**	C	^1A	C_1	5.84	−2.83
5I	R	$^1A_1'$	D_{5h}	6.46	−0.13	**10I**	C	^1A	C_2	6.42	−1.91
6II	R	$^1A_{1g}$	D_{6h}	6.28	0.09	**10II**	C	^1A	C_3	6.36	−2.76
7III	R	^1A	D_{7h}	6.36	0.09	**10III**	C	^1A_g	C_{2h}	6.28	−3.56
8V	R	$^1A_{1g}$	D_{8h}	6.29	0.08	**10IV**	C	$^1A'$	C_s	3.47	−1.58
9V	R	^1A	D_{9h}	6.37	0.07	**11I**	C	$^1A'$	C_s	6.45	−2.03
4II	DR	$^1A_1$	T_d	5.76	−10.09	**11II**	C	$^1A'$	C_s	6.41	−1.55
6I	DR	$^1A_{1g}$	D_{3d}	6.33	−3.82	**11III**	C	^1A	C_1	6.34	−1.41
8II	DR	$^1A_1$	D_{4d}	6.54	−1.58	**11IV**	C	^1A	C_1	5.93	−2.13
10V	DR	$^1A_{1g}$	D_{5d}	6.54	−0.86	**12II**	C	$^1A_1$	D_3	6.43	−1.92
9IV	TR	$^1A_1'$	D_{3h}	6.14	−3.29	**12I**	F	^1A_g	T_h	6.86	−1.41
12IV	TR	$^1A_{1g}$	D_{4h}	5.72	−0.95	**16I**	F	$^1A_1$	T_d	6.77	−0.77
12III	QR	$^1A_{1g}$	D_{3d}	6.28	−2.13	**20I**	F	^1A_g	C_{4h}	6.83	−1.25
7II	C	$^1A_1$	C_{3v}	5.96	−3.58	**24I**	F	$^1A_1$	O	7.38	−0.57

[a]The structures divided into different families: R (rings), DR (double rings), TR (triple rings), QR (quad-rings), C (cages), and F (fullerenes).
[b]Electronic state.
[c]Point group (symmetry).
[d]Energy gaps (eV) between the highest occupied molecular orbit and lowest unoccupied molecular orbit.
[e]Nucleus independent chemical shift values (ppm) in cluster centers at the TPSSh/6-311+G* level.

Figure 3(b) in a manner that emphasizes particular stable minima or "magic numbers." In such a curve, downward peaks represent that the energy is lower than the average and the structure is the most stable magic number ($N = 4$, 9, 12 as shown in the figure). For the magic numbers, not only the energy gaps between the GMs and the second isomer are large (1.58, 1.16, and 2.42 eV for $N = 4$, 9, and 12, respectively), but also they have high geometric symmetry (D_{4h}, C_{3h}, and T_h, respectively).

Figure 4 plots energies between the lowest-energy structures of different families. At small sizes (n ≤ 5), monocyclic rings are much lower in energy than other packings. Then, with the cluster size increasing, at $N = 6$ and 7, the global minimum structures are dominated by the three-dimensional double rings. Energy gaps of the three packings are small (especially for $(BeO)_7$, the energy gap between the GM and third lowest energy structure is only 0.32 eV). When $N \geq 8$, the GMs are cages, and multi-rings are the second lowest energy structural families, but monocyclic rings and cubic are much disfavored in energy.

Additionally, the energy gap (Δ_{HL}) between the highest occupied molecular orbit and lowest unoccupied molecular orbit is an important factor influencing the structural

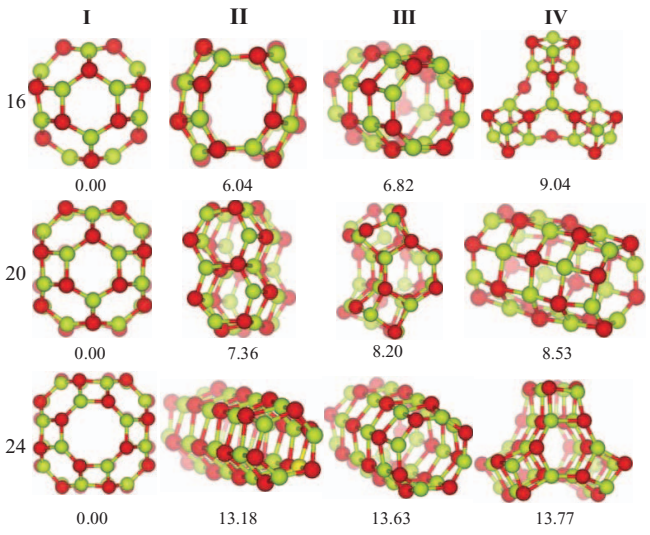

FIG. 2. Relevant structures of $(BeO)_N$ of $N = 16$, 20, and 24. The structures in column **I** correspond to the global minima; columns **II**–**V** correspond to isomers (local minima) that are higher in energy, and the relative energies in eV are labeled in figure. O-red; Be-green.

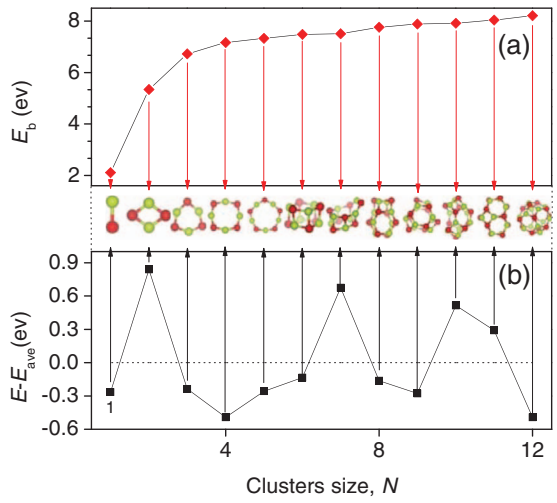

FIG. 3. (a) Binding energy per BeO unit (E_b) of BeO clusters as a function of cluster size N, where $E_b = E(Be) + E(O_2/2) - E(Be_NO_N)/N$; (b) Plots of the energetic gaps ($E - E_{ave}$) of the GMs as a function of cluster size, where E is the total energy, and E_{ave} is a four-parameter fit of the GMs: $E_{ave} = 43.68998 - 75.73901*N^{1/3} + 48.92967*N^{2/3} - 2463.84458*N$. Downward peaks represent the most stable magic numbers compared to the neighbors. The GM structures are also labeled.

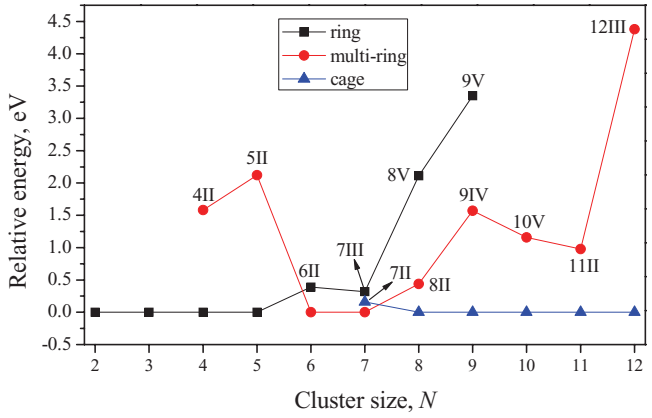

FIG. 4. Relative energies between the lowest-energy structures of different families (rings, multi-rings, and cages) as a function of the cluster size.

stability. Beryllium oxide is a kind of direct gap metal oxide, and its Δ_{HL} is relatively large. Clusters inherit these properties of bulk, the Δ_{HL} of all structures (except for 2**I** and 10**IV**) are large (5.72–7.38 eV). 2**I** and 10**IV** have relatively small Δ_{HL} (3.99 and 3.47 eV), which result from the instability of their geometries (the rhombic unit is too strained).

C. Aromaticity

It is known that aromatic character is a useful quantity in stability and reactivity of many molecules.[27,28] The nucleus independent chemical shifts (NICS) value is a popular magnetic criterion of aromacitity.[29] Table II gives the NICS value at the center of isomers for BeO clusters. The results indicate that most of the isomers are aromatic, only a few isomers are non-aromatic, but none of them is anti-aromatic. Besides, we note that all GMs of $(BeO)_N$ clusters are aromatic based on NICS values.

Small rings (2**I**, 3**I**, 4**I**, and 5**I**) are aromatic (NICS = −10.67, −6.44, −0.99, and −0.13 ppm), but the large rings (6**II**, 7**III**, 8**V**, and 9**V**) are non-aromatic (the NICS = 0.09, 0.09, 0.08, and 0.07 ppm, respectively). Possible reason is that electric delocalization is harder at a larger ring. Double-, triple-, and quad-ring structures 4**II**, 6**I**, 7**I**, 8**II**, 10**V**, 9**IV**, 12**III**, and 12**IV** are all aromatic, among which 4**II** is the most aromatic one (NICS = −10.09 ppm). All cages 7**II**, 8**I**, 9**I**, 9**II**, 10**I**, 10**II**, 10**III**, 10**IV**, 11**I**, 11**II**, 11**III**, and 11**IV** are also aromatic (NICS = −1.4 to −3.6 ppm). Similar to other fullerene-like structure,[30] 12**I**, 16**I**, 20**I**, and 24**I** are aromatic too (NICS = −1.41, −0.77, −1.25, and −0.57 ppm, respectively). Summarily, the majority of low-lying isomers are aromatic, and only several large rings are non-aromatic. This is different from $(BN)_N$ clusters, $(BN)_N$ rings with odd values of N are aromatic, but those with even values of N are anti-aromatic, except for $N = 2$.[4]

D. Bonding patterns

Due to the particularity of Be–O bond, it is necessary to investigate the bonding features of $(BeO)_N$ clusters. Adaptive natural density partitioning (AdNDP) is a new theoretical tool

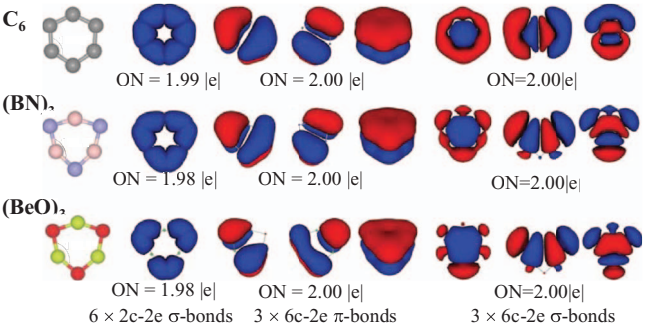

FIG. 5. Comparisons of structures and AdNDP bonding patterns (molecular orbits) for C_6, $(NB)_3$, and $(BeO)_3$ rings. ON correspond to the occupation number; 2c-2e (two-center two-electron), 6c-2e (six-center two-electron); C-gray, N-blue, B-pink, Be-green, O-red.

for analysis of chemical bonding.[31] This approach provides partitioning of the charge density into elements with the high-possible degree of localization of electron pairs such as the n-center two-electron (nc-2e) bonds, including core electrons, lone pairs, 2c-2e bonds and so on. AdNDP has been successfully applied to the analysis of chemical bonds in clusters[31–33] and organic aromatic molecules.[34] $(BeO)_3$ is isoelectronic with C_6 and $(BN)_3$, owning 24 valence electrons. The GMs are six-membered rings with D_{3h} symmetry.[4,35] Figure 5 plots the comparisons of the structures and AdNDP bonding patterns for $(BeO)_3$, C_6, and $(BN)_3$ rings. AdNDP analysis reveals that they have similar bonding patterns. There are six 2c-2e σ-bonds (superimposed on the single molecular framework), three 6c-2e π-bonds, and three 6c-2e σ-bonds. According to Huckel's $4n + 2$ rule for aromaticity, C_6, $(BN)_3$, and $(BeO)_3$ are doubly aromatic with 6 delocalized π electrons (3 π orbits) and 6 delocalized σ electrons. The degree of the electron delocalization decreases from C_6 to $(BN)_3$ to $(BeO)_3$.

C_{24} and $(BeO)_{12}$ are both fullerene-like structures. The comparison for AdNDP bonding patterns between C_{24} and $(BeO)_{12}$ is pretended in Figure 6. The AdNDP analysis shows that their bonding patterns are similar, including two kinds

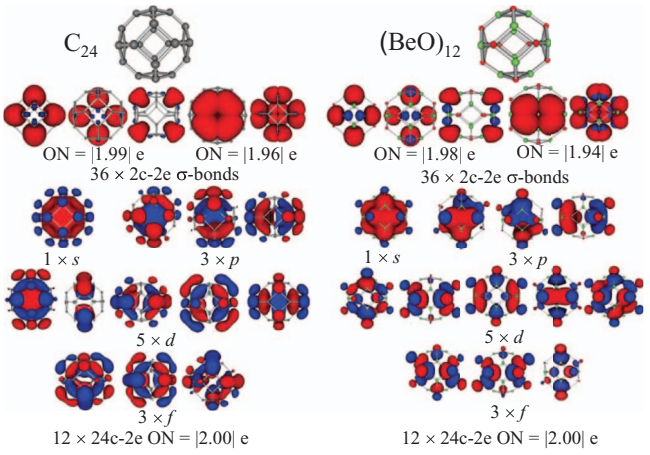

FIG. 6. Comparisons of structures and AdNDP bonding patterns (molecular orbits) for C_{24} and $(BeO)_{12}$ fullerenes. ON correspond to the occupation number; 2c-2e (two-center two-electron), 24c-2e (twenty four-center two-electron); C-gray, O-red, Be-green.

of σ-bonds (one belongs to four-membered rings, and another belongs to six-membered rings). There are 36 2c-2e σ-bonds (occupation number (ON) = 1.99−1.96 |e| for C_{24} and 1.99−1.96 |e| for $(BeO)_{12}$, superimposed on the single molecular framework). The remaining 24 electrons shared by the entire fullerene, forming the molecular orbits, which can be treated as: one *s*-orbit, three *p*-orbits, five *d*-orbits, and three *f*-orbits (Figure 6). The AdNDP analysis predicts that $(BeO)_{12}$ is also a fullerene.

E. Discussion

BeO is isoelectronic with C_2, BN, and LiF. There are differences and similarities in structures for C, BN, BeO, LiF, and MgO clusters. Many of the low-lying structures (especially for BeO, LiF, and MgO) are similar to each other. From C to BN to BeO to LiF, the ionicity of bond between two atoms increases, and the covalency decreases gradually. Their cluster structures gradually transform from 2D to 3D (cage and cubic). Carbon, boron, and nitrogen are in sp^2 hybridization, small carbon and BN clusters are in favor of planar and cage structures. LiF and MgO are ionic compounds, their crystals are cubic structures. Alkaline earth oxides except for beryllium oxide are ionic compounds. Polarization capability of beryllium ion is the strongest in alkaline earth metals, beryllium oxides can be regarded as covalent compound with certain characteristics of ionic bond. Based on this characteristic of Be–O bond (between the ionic and covalent bond), BeO cluster is a transition from covalent (C and BN) to ionic (LiF and MgO) clusters. Additionally, the characteristics result in the structural difference between beryllium oxides and other alkaline earth oxides clusters. For example, the GMs of $(MgO)_N$ clusters are monocyclic rings at $N = 2$ and 3, double rings at $N = 4$–6, cages at $N \geq 7$, and cubic at very large size. The particularity of Be–O bond makes BeO clusters have unique structures and properties. Special structures would be potentially applicable in ceramic material and the field of rock and aviation.

IV. CONCLUSION

The structures for $(BeO)_N$ ($N = 2$–12, 16, 20, 24) clusters are investigated using the combination of genetic algorithm and DFT method (TPSSh functional). A lot of relevant low-lying structures are obtained. The global minimum structures are monocyclic rings up to $N = 5$, double rings at $N = 6$ and 7, cages at $N \geq 8$, among which $(BeO)_N$ ($N = 4$, 9, and 12) are the most stable magic numbers. The majority of structures of BeO clusters are aromatic according to nucleus independent chemical shifts criterion. AdNDP analysis shows that C_6, $(BN)_3$, and $(BeO)_3$ rings (C_{24} and $(BeO)_{12}$ fullerenes) are similar in bonding patterns. The building-up principle of $(BeO)_N$ is different from that of covalent (BN) and ionic (LiF and MgO) clusters. At very large size, $(MgO)_N$ and $(LiF)_N$ favor cubic (consistent with their crystal structure). However, the structures of $(BeO)_N$ clusters at large sizes are still in favor of cages.

ACKNOWLEDGMENTS

This work is supported by the National Natural Science Foundation of China (NNSFC) (20903001), by the 211 Project and by the outstanding youth foundation of Auhui University. The calculations are carried out on the High-Performance Computing Center of Anhui University. We acknowledge Professor Boldyrev for the AdNDP codes.

[1] M. L. Cohen, Nature (London) **338**, 292 (1989).
[2] M. Jansen, Angew. Chem., Int. Ed. **41**, 3766 (2002).
[3] R. Ferrando, J. Jellinek, and R. L. Johnston, Chem. Rev. **108**, 845 (2008).
[4] J. M. Matxain, J. M. Ugalde, M. D. Towler, and R. J. Needs, J. Phys. Chem. A **107**, 10004–10010 (2003).
[5] A. Aguado and J. M. López, J. Phys. Chem. B **104**, 8398–8405 (2000).
[6] X. Ding, W. Xue, Y. Ma, Z. Wang, and S. He, J. Chem. Phys. **130**, 014303 (2009).
[7] S. Darby, T. V. Mortimer-Jones, R. L. Johnston, and C. Roberts, J. Chem. Phys. **116**, 1536–1550 (2002).
[8] R. A. Lordeiro, F. F. Guimarães, J. C. Belchior, and R. L. Johnston, Int. J. Quantum Chem. **95**, 112–125 (2003).
[9] N. T. Wilson and R. L. Johnston, J. Mater. Chem. **12**, 2913–2922 (2002).
[10] M. S. Bailey, N. T. Wilson, C. Roberts, and R. L. Johnston, Eur. Phys. J. D **25**, 41–55 (2003).
[11] F. Chen, B. C. Curley, G. Rossi, and R. L. Johnston, J. Phys. Chem. C **111**, 9157–9165 (2007).
[12] F. Chen and R. L. Johnston, ACS Nano **2**, 165–175 (2007).
[13] C. Wang, Z. Du, X. Huang, X. Duan, and M. Li, Int. Mater. Rev. **25**, 123–126 (2011).
[14] M. J. Frisch, G. W. Trucks, H. B. Schlegel *et al.*, GAUSSIAN 09, Revision B.01, Gaussian, Inc., Wallingford, CT, 2009.
[15] J. Tao, J. P. Perdew, V. N. Staroverov, and G. E. Scuseria, Phys. Rev. Lett. **91**, 146401 (2003).
[16] C. Adamo and V. Barone, J. Chem. Phys. **110**, 6158–6170 (1999).
[17] Y. Zhao and D. G. Truhlar, J. Chem. Phys. **125**, 194101 (2006).
[18] A. D. Becke, J. Chem. Phys. **98**, 5648–5652 (1993).
[19] W. B. Smith, Magn. Reson. Chem. **37**, 103–106 (1999).
[20] J. P. Perdew, J. A. Chevary, S. H. Vosko, K. A. Jackson, M. R. Pederson, D. J. Singh, and C. Fiolhais, Phys. Rev. B **48**, 4978–4978 (1993).
[21] K. P. Jensen, B. O. Roos, and U. Ryde, J. Chem. Phys. **126**, 014103 (2007).
[22] J. P. Perdew, Phys. Rev. B **33**, 8822–8824 (1986).
[23] G. D. Purvis and R. J. Bartlett, J. Chem. Phys. **76**, 1910–1918 (1982).
[24] K. Doll, J. C. Schön, and M. Jansen, J. Chem. Phys. **133**, 024107 (2010).
[25] K. Kwapien, M. Sierka, J. Dobler, J. Sauer, M. Haertelt, A. Fielicke, and G. Meijer, Angew. Chem., Int. Ed. **50**, 1716–1719 (2011).
[26] R. Dong, X. Chen, X. Wang, and W. Lu, J. Chem. Phys. **129**, 044705–044705 (2008).
[27] F. De Proft and P. Geerlings, Chem. Rev. **101**, 1451–1464 (2001).
[28] A. R. Katritzky, M. Karelson, S. Sild, T. M. Krygowski, and K. Jug, J. Org. Chem. **63**, 5228–5231 (1998).
[29] P. v. R. Schleyer, C. Maerker, A. Dransfeld, H. Jiao, and N. J. R. v. E. Hommes, J. Am. Chem. Soc. **118**, 6317–6318 (1996).
[30] V. Elser and R. C. Haddon, Nature (London) **325**, 792–794 (1987).
[31] D. Y. Zubarev and A. I. Boldyrev, Phys. Chem. Chem. Phys. **10**, 5207–5217 (2008).
[32] D. Y. Zubarev and A. I. Boldyrev, J. Phys. Chem. A **113**, 866–868 (2008).
[33] L. Cheng, J. Chem. Phys. **136**, 104301 (2012).
[34] D. Y. Zubarev and A. I. Boldyrev, J. Org. Chem. **73**, 9251–9258 (2008).
[35] K. Raghavachari, R. Whiteside, and J. Pople, J. Chem. Phys. **85**, 6623 (1986).